The Research Council of Norway (NFR)

NORSAR

NORSAR Scientific Report No. 1-97/98

Semiannual Technical Summary

1 April – 30 September 1997

Kjeller, November 1997

7.2 Status of the global Threshold Monitoring (TM) system

Introduction

Detailed descriptions of the global Threshold Monitoring (TM) system have been given in several of the latest NORSAR Semiannual Technical Summaries (Kværna et al., 1994, Ringdal et al., 1995, Kværna, 1996, 1997), and for information on the technical details we refer to these reports and the references therein. In this report we will give the status of the development and testing of the TM system at the Provisional International Data Center (PIDC), as well as outlining some of our ideas for future development of the system.

Continuous TM processes

During the 6 months of this reporting period we have been running all the basic computational processes of the TM system on the PIDC testbed. These processes are:

- Continuous calculation of short-term-averages (STAs) for all primary stations using the detection and feature extraction program (*DFX*) running in the Alpha processing pipeline. The STAs are written to cyclical files for subsequent usage. The processes in the Alpha pipeline are running as close as possible to real-time.
- Continuous calculation of the three-station detection capability of the network for a set of 2562 globally distributed target areas, using the STAs calculated by *DFX*. This program, called *tm_regproc*, is implemented in the Delta processing pipeline, running with a delay of 10 hours behind real-time.
- Interpolation and reformatting of the three-station detection capability to facilitate map displays of the results. This program, called *tm_data2rdf*, is also implemented in the Delta pipeline.

These processes have all been running without errors, and they have not caused any problems to the continuous operation of the PIDC testbed. In addition, we have verified that the computational resources available at the PIDC testbed are sufficient for keeping the TM related processes up with real-time. This shows that the basic computational processes of the TM system are now of sufficient quality to satisfy the requirements for transfer into the operational pipeline at the PIDC.

TM Products

A set of programs for generation of products from the TM system was implemented on the PIDC testbed in mid-September, but due to some problems with the operational environment, we initially faced some difficulties in getting our programs into stable operation. We now hope to have identified the main problems, and anticipate that with the latest changes to our programs, stable operation can be accomplished.

Three types of products (plots) are now available from the TM system. These products are designed to provide useful information to the international community on the performance and status of the primary seismic network used for monitoring of the Comprehensive Test Ban

Treaty (CTBT). All of these plots are created on an hourly basis and provide an overview of the characteristics of the primary seismic network during the analyzed hour.

In the following, a detailed description of the different products will be given:

Information on data availability and seismic events

There are four main factors that cause variations in the event detectability of the primary seismic network. These are:

- Fluctuations with time in the background noise level
- Changes in data quality at the PIDC caused by communications problems, station outages or other data errors like spikes and gaps
- Temporary deficiencies in the PIDC data processing
- Signals from interfering seismic events around the world.

For the first type of hourly plots, shown in Fig. 7.2.1, the color of the station symbols provide information on the availability of data for a particular 1-hour interval (1997/09/07 10:00 to 11:00). The arrays are marked by circles and three-component stations by triangles. Red symbols indicate that data were successfully recorded and processed less than 10% of the total time interval, yellow symbols indicate a success rate between 10% and 90% and green symbols indicate that for more than 90% of the time data were successfully recorded and processed.

In order to estimate the detection capability at different parts of the world for a 1 hour interval, we need to take into account the maximum travel-time of the phases possibly originating anywhere in the Earth within this time interval. This means that with the current parametrization of the TM system, we actually need to analyze about 1 hour and 22 minutes of data from each station, and the statistics shown in Fig. 7.2.1 in fact apply to this interval.

The statistics on available and processed data is derived from the short-term-averages (STAs) of the different stations, and the STAs of the cyclical files are assigned particular null values if there are gaps in the processing by DFX. Processing gaps are reported in the cases of unavailable data or processing problems at the PIDC, or if the data quality checking feature of DFX identified erroneous data so that DFX was unable to create STA traces.

Notice that for the interval reported in Fig. 7.2.1, the Australian arrays (ASAR and WRA), the GERES and FINES arrays in Europe, as well as the BGCA and partly the DBIC stations in Africa were all down. As shown later in this report, the outage of ASAR and WRA lead to a significantly reduced event detection capability for the areas within and around Australia.

When the Reviewed Event Bulletin (REB) is complete, the locations of events originating within or close to the actual time interval are introduced into these plots, and the event information are given below the map (see Fig. 7.2.1.). Notice the occurrence of a major event (m_b 4.9) and an aftershock in Pakistan.

Detailed information on station outages and processing gaps, arriving signals and fluctuations in the background noise level

The panel shown in Fig.7.2.2 provides an overview of the background noise level and the observed signals at each of the primary stations during the data interval (1 hr 22 min 20 s) used for assessing the detection capability of the 1 hour interval.

The traces shown are continuous log (A/T) equivalents derived from the STA traces. The STA traces are calculated from filtered beams for the arrays, and for the three-component stations from filtered vertical-component channels.

The fluctuations in the log(A/T) equivalents are either caused by variations in the background noise levels, calibration signals, data problems like unmasked spikes or electronic noise, or signals from seismic events. Notice in particular the signals from the m_b 4.9 event in Pakistan (origin time 10:15:24) seen at most stations of the primary network.

For each station, the cutoffs of the filter bands used for teleseismic monitoring are given below the station codes. Also given are the average values of the log(A/T) equivalents, which is an overall measure of the background noise level. Generally speaking, a low background noise level indicate a good capability to detect signals, and vice versa.

The percentages of successfully recorded and processed data are also given for each station, and the intervals with gaps in data processing are indicated in red above the time axis.

Together with the station and event information illustrated in Fig. 7.2.1, the station data panel shown in Fig. 7.2.2 provide a convenient tool for assessing the state-of-health of the PIDC primary seismic network. In addition, this information will help to explain temporary variations in the global event detectability.

Network detection capability maps

As presented in the previous Semiannual Technical Summary (Kværna, 1997), a simplified instantaneous network detection capability map can be computed by choosing the **third lowest** of the station "noise magnitudes", and then adding e.g., 0.7 m_b units to accommodate an SNR of 5.0 required for phase detection.

As a product from the global Threshold Monitoring system, we show in the upper map of Fig. 7.2.3 the average network detection capability for the 1-hour interval (1997/09/07 10:00 to 11:00). Variation from hour to hour of the average detection capability is primarily caused by long station or processing outages, by increased background noise levels at the different stations, or by signals of longer duration from large seismic events. Notice in particular the low detection capability around Australia and Africa caused by the outages of the stations ASAR, WRA, BGCA and partly DBIC.

In addition, the lower map of Fig 7.3.3 shows the poorest (lowest) detection capability for the analyzed hour. Differences from the average capability are primarily caused by signals from seismic events, shorter outages, and data errors like unmasked spikes or electronic noise.

Notice that the m_b 4.9 event in Pakistan temporarily lowers the detection capability all over the world, in particular in the neighborhood of the actual event location.

Both types of maps shown in Fig. 7.2.3 should provide important information on the capability of the primary seismic network to detect events in different parts of the world, whereas the information provided in Figs. 7.2.1 and 7.2.2 will help to explain the variations in the global event detection capability.

The products provided from the global TM system should in this way be useful for monitoring compliance with the CTBT, in particular by placing confidence on the performance of the International Monitoring System, but also by giving a warning in the case of lowered monitoring capability, e.g., caused by station outages, communication problems, data processing problems or extremely high seismic activity.

Transfer of the Global Threshold Monitoring system from the PIDC testbed to the PIDC operational pipeline

Although the testing of the different modules of the TM system are approaching its completion on the PIDC testbed, there is some work left before we are ready to move the TM system to the operational pipeline. During the next couple of months we therefore have to focus on completing the operational and users' manual as well as streamlining the different scripts and programs for operation by non-expert users. Once this is completed a proposal will be written to the PIDC Configuration Control Board (CCB) for transfer of the TM system to the PIDC operational pipeline.

Future developments

We plan in the near future to include in the TM system the bulk station magnitude corrections derived from the event station magnitudes reported in the Reviewed Event Bulletins (REBs). This will require little work, but it will significantly reduce the uncertainty associated with the estimated global detection capability.

The threshold monitoring concept was originally developed to assess the maximum magnitude of possibly hidden events in given regions, at the 90% confidence level (Ringdal and Kværna, 1989, 1992). With this approach we also obtain an estimate of the monitoring capability of the network to observe small events in different target areas using the most sensitive stations of the network. Somewhat simplified, we could say that for events below the monitoring threshold, it would be unlikely to observe signals at any stations of the network. On the other hand, for event magnitudes slightly above the monitoring threshold, it may be possible to observe signals at the most sensitive stations of the network by visual inspection or by running a detector at a low detection threshold.

The upper map of Fig. 7.2.4. shows the average monitoring threshold for the 1-hour interval (1997/09/07 10:00 to 11:00). Notice that in North America and northern Europe the average monitoring threshold is very low due to the location of sensitive array stations located in these regions, whereas the monitoring threshold around Africa and Australia is high because of station outages.

It seems that the average monitoring threshold is generally about one magnitude unit lower than the average three-station detection capability shown in Fig. 7.2.3. This means that by reanalyzing data at the stations most sensitive to events in a given region, we are able to observe signals from events with magnitudes significantly below the number given by the three-station detection capability. Notice that the color code is shifted by 0.5 m_b units between Figs. 7.2.3 and 7.2.4.

Similar to the poorest detection capability shown in the lower map of Fig 7.2.3, the lower map of Fig. 7.4.4 shows the highest monitoring threshold during the analyzed hour. Again, notice the temporary increase in monitoring threshold for large parts of the world caused by signals from the m_b 4.9 event in Pakistan.

We may at a later stage include the maps of the average and highest monitoring threshold as a product from the global TM system. The monitoring thresholds will provide information as to what extent it is possible, at a later stage, to identify signals from smaller seismic events that were not reported in the Reviewed Event Bulletin. This suggests that the low monitoring thresholds obtainable by TM system could have a significant deterrence value during a CTBT.

T. Kværna
F. Ringdal
U. Baadshaug
H. Iversen

References

Kværna, T., F. Ringdal, H. Iversen and N.H.K. Larsen (1994): A system for continuous seismic threshold monitoring, final report, Semiannual Tech. Summ., 1 Apr - 30 Sep 1994, NORSAR Sci. Rep, 1-94/95, NORSAR, Kjeller, Norway

Kværna, T. (1996): Tuning of processing parameters for Global Threshold Monitoring at the IDC, Semiannual Tech. Summ., 1 Apr - 30 Sep 1996, NORSAR Sci. Rep, 1-96/97, NORSAR, Kjeller, Norway

Kværna, T. (1997): Threshold magnitudes, Semiannual Tech. Summ., 1 Oct 1996 - 31 Mar 1997, NORSAR Sci. Rep, 2-96/97, NORSAR, Kjeller, Norway

Ringdal, F. and T. Kværna (1989): A multi-channel approach to real time network detection, location, threshold monitoring. *Bull. Seism. Soc. Am.*, 79, 1927-1940.

Ringdal, F. and T. Kværna (1992): Continuous seismic threshold monitoring, *Geophys. J. Int.*, 111, 505-514.

Ringdal, F., T. Kværna and S. Mykkeltveit (1995): Global seismic threshold monitoring and automated network processing, Semiannual Tech. Summ., 1 Oct 1994 - 31 Mar 1995, NORSAR Sci. Rep, 2-94/95, NORSAR, Kjeller, Norway

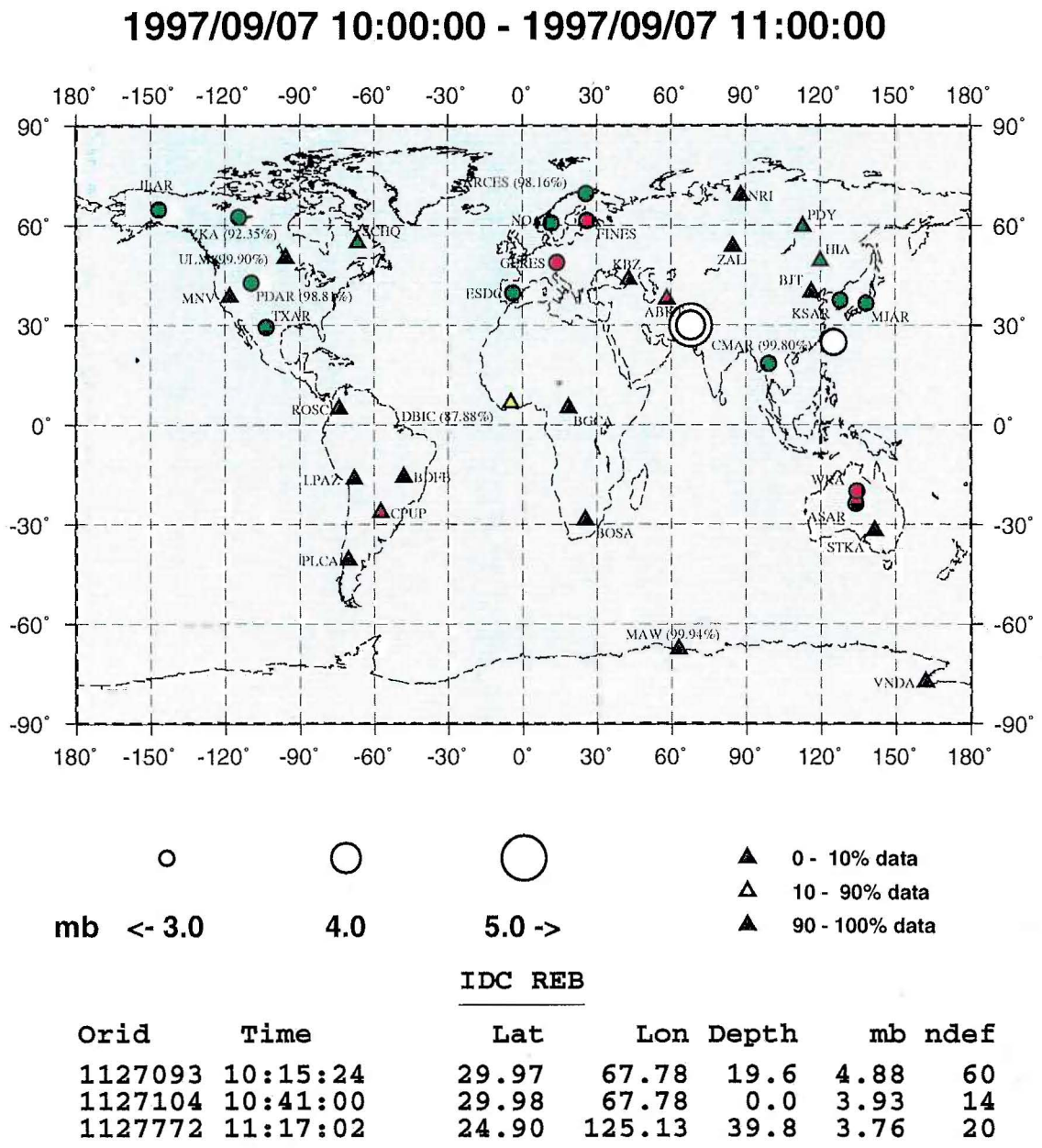

IDC REB

Orid	Time	Lat	Lon	Depth	mb	ndef
1127093	10:15:24	29.97	67.78	19.6	4.88	60
1127104	10:41:00	29.98	67.78	0.0	3.93	14
1127772	11:17:02	24.90	125.13	39.8	3.76	20

Figure 7.2.1. *The color of the station symbols provide information on the availability of data for a particular 1-hour interval (1997/09/07 10:00 to 11:00). The arrays are marked by circles and three-component stations by triangles. Red symbols indicate that data were successfully recorded and processed less than 10% of the total time interval, yellow symbols indicate a success rate between 10% and 90% and green symbols indicate that for more than 90% of the time data were successfully recorded and processed.*

Notice that for the interval reported, the Australian arrays (ASAR and WRA), the GERES and FINES arrays in Europe, as well as the BGCA and partly the DBIC stations in Africa were all down.

When the Reviewed Event Bulletin (REB) is complete, the locations of events originating within or close to the actual time interval is plotted, and the event information is given below the map. Notice the occurrence of a major event (m_b 4.9) and an aftershock in Pakistan.

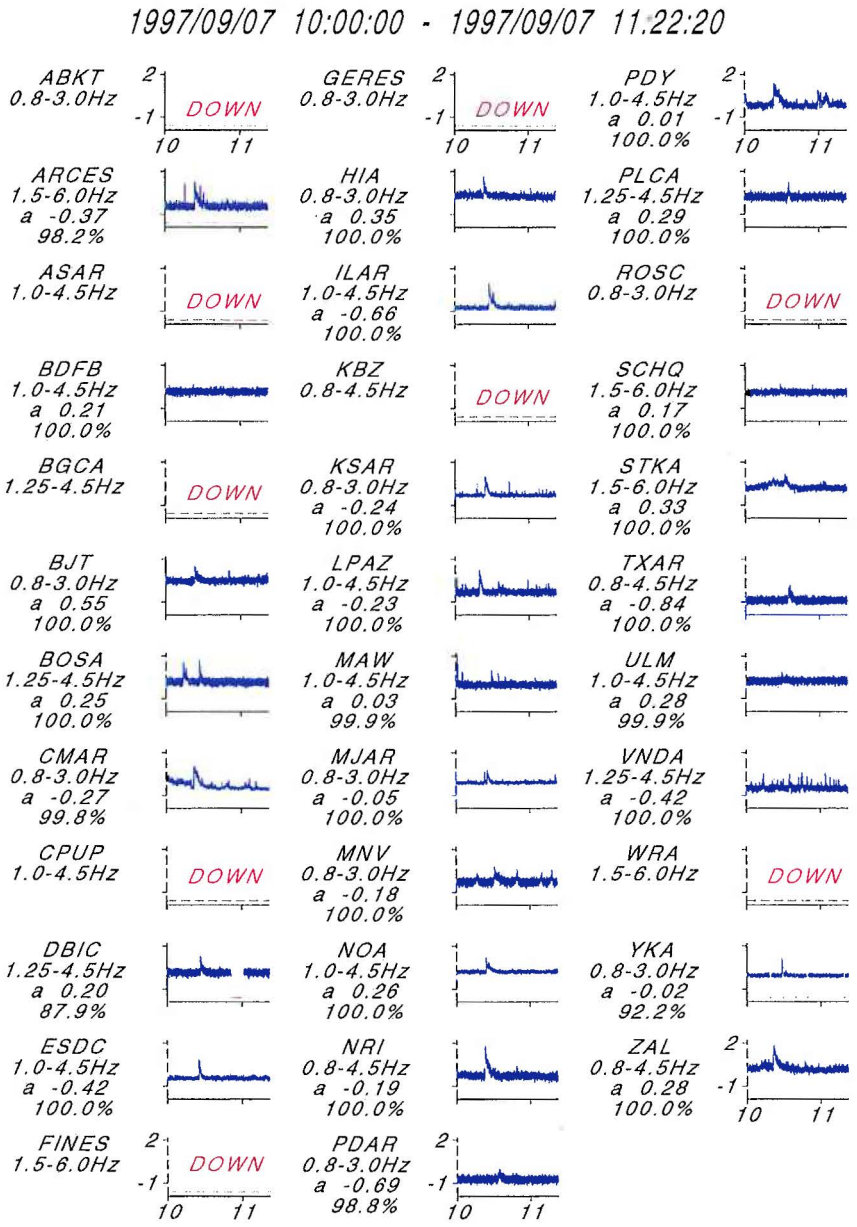

Figure 7.2.2. *The panel provides an overview of the background noise level and the observed signals at each of the primary stations during the data interval (1 hr 22 min 20 s) used for assessing the detection capability of the 1 hour interval. The traces shown are continuous log (A/T) equivalents derived from the STA traces. Notice in particular the signals from the m_b 4.9 event in Pakistan (origin time 10:15:24) seen at most stations of the primary network.*

The STA traces are calculated from filtered beams for the arrays, and for the three-component stations from filtered vertical-component channels. For each station, the cutoffs of the filter bands used for teleseismic monitoring are given below the station labels. Also given are the average values of the log(A/T) equivalents, which is an overall measure of the background noise level.

The percentages of successfully recorded and processed data are also given for each station, and the intervals with gaps in data processing are indicated in red above the time axis.

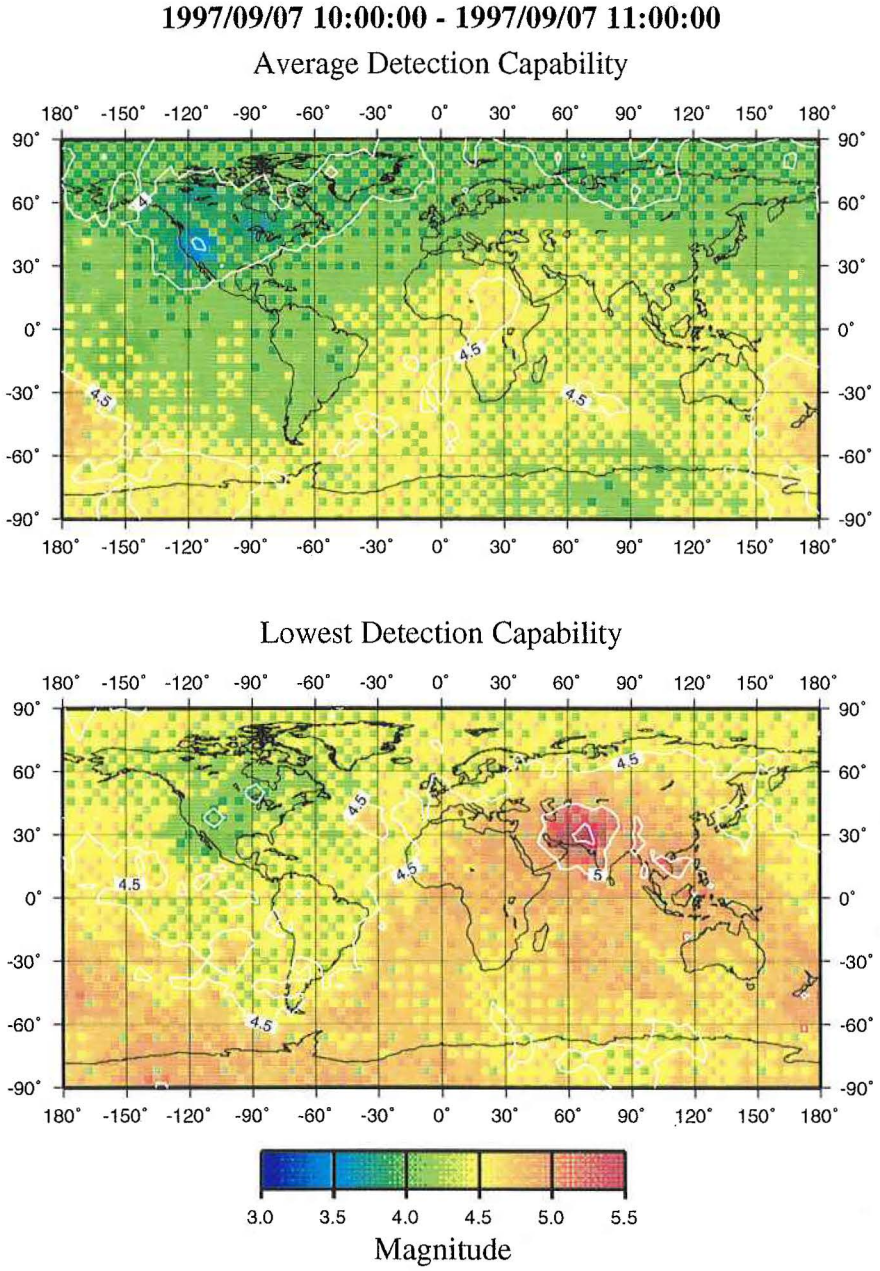

Figure 7.2.3. *The the upper map of the figure shows the average network detection capability for the 1-hour interval (1997/09/07 10:00 to 11:00). Variation from hour to hour of the average detection capability is primarily caused by longer station or processing outages, by increased background noise levels at the different stations, or by signals of long duration from large seismic events. Notice in particular the low detection capability around Australia and Africa caused by the outages of the stations ASAR, WRA, BGCA and partly DBIC.*

The lower map shows the poorest (lowest) detection capability for the analyzed hour. Differences from the average capability are primarily caused by signals from seismic events, shorter outages, and data errors like unmasked spikes or electronic noise. Notice that the m_b 4.9 event in Pakistan temporarily lowers the detection capability all over the world, and in particular in the neighborhood of the actual event location.

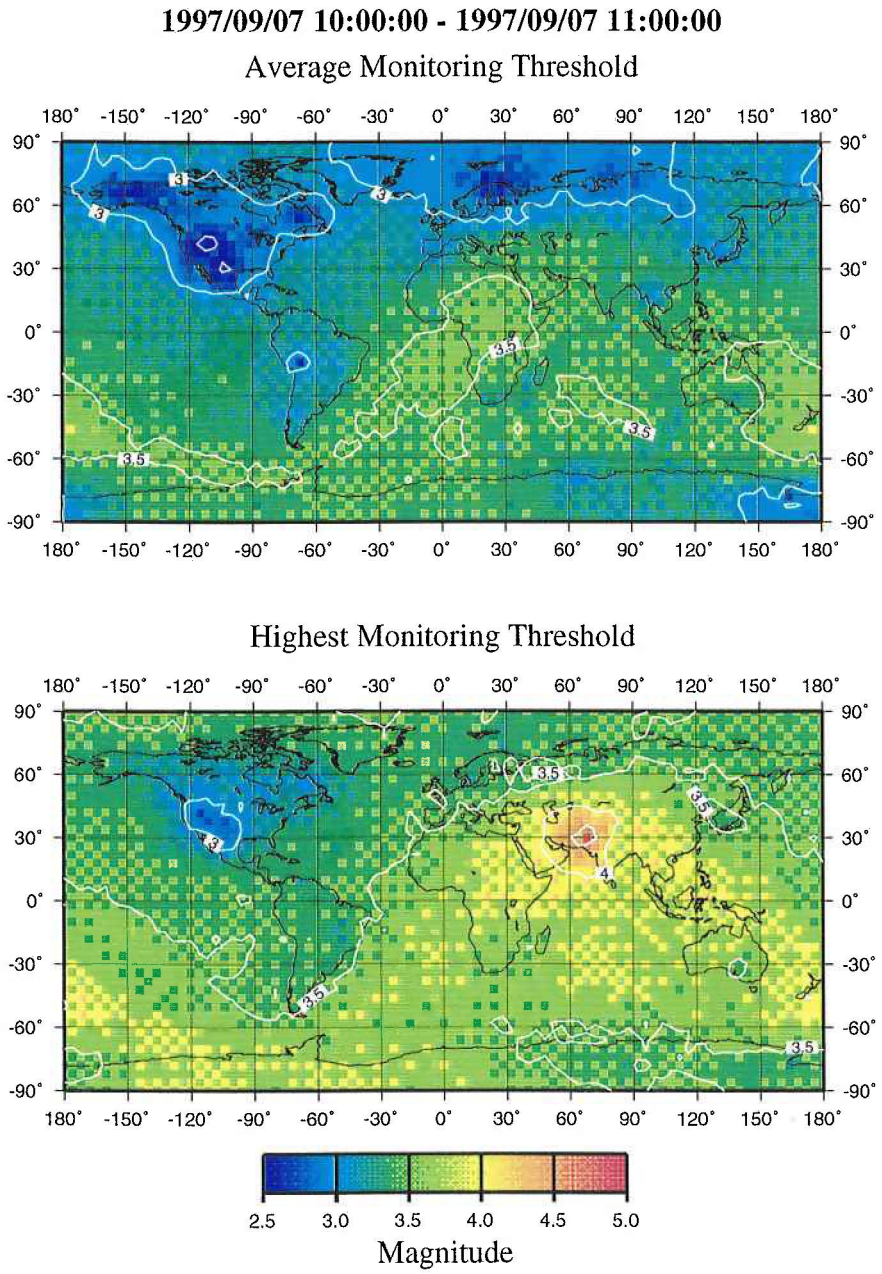

Figure 7.2.4. *The upper map shows the average monitoring threshold for the 1-hour interval (1997/09/07 10:00 to 11:00). The monitoring threshold gives an estimate of the monitoring capability of the network to observe small events in different target areas using the most sensitive stations of the network.*

Notice that in North America and northern Europe the average monitoring threshold is very low due to the location of sensitive array stations located in these regions, whereas the monitoring threshold around Africa and Australia is high because of station outages.

It seems that for the current primary seismic network, the average monitoring threshold is generally about one magnitude unit lower than the average three-station detection capability shown in Fig. 7.2.3. This means that by reanalyzing data at the stations most sensitive to

events in a given region, we are able to observe signals from events with magnitudes significantly below the number given by the tree-station detection capability. Notice that the color code is shifted by 0.5 m_b units between Figs. 7.2.3 and 7.2.4.

Similar to the poorest detection capability shown in the lower map of Fig 7.2.3, the lower map of this figure shows the highest monitoring threshold during the analyzed hour. Again, notice the temporary increase in monitoring threshold for large parts of the world caused by signals from the m_b 4.9 event in Pakistan.